J. Membrane Biol. 82, 221–239 (1984)

The Journal of
Membrane Biology

Slow Potential Changes Due to Transport Number Effects in Cells with Unstirred Membrane Invaginations or Dendrites

Peter H. Barry
Nerve-Muscle Research Centre, School of Physiology and Pharmacology, University of New South Wales, Kensington, Australia

Summary. Many neurones are extremely invaginated and possess branching processes, axons and dendrites. In general, they are surrounded by a restricted diffusion space. Many of these cells exhibit large, slow potential changes during the passage of current across their membranes. Whenever currents cross membranes separating aqueous solutions, differences in transport numbers of the major permeant ions give rise to local concentration changes of these ions adjacent to the membranes, which will result in various electrical and osmotic effects. These transport number effects are expected to be enhanced by the presence of membrane invaginations. Dendrites are equivalent to reversed invaginations and there should be significant changes in concentrations of permeant ions within them. In general, the effects of such changes on the electrical response of a cell will be greater when the concentration of a major permeant ion is low. The effects have been modelled in terms of two nondimensional parameters: the invagination transport number parameter β and the relative area occupied by the invaginations δA. If these two parameters are known, the magnitudes and time course of the slow potential changes can immediately be estimated and the time course converted to real time, if the length of the invaginations (ℓ) and ionic diffusion coefficient (D) within them are also known. Both analytical and numerical solutions have been given and predictions compared. It is shown that in the case of large currents and potentials the analytical solution predictions will underestimate the magnitudes and rates of onset of the voltage responses. The relative magnitude of the transport number effect within the invaginations (or dendrites) and other transport number contributions to slow potential changes have also been assessed and order-of-magnitude values of these are estimated for some biological data.

Key Words transport number effects · membrane invaginations · dendrites · restricted diffusion space · slow potential changes · slow conductance changes · neurones · solute polarization · membrane infoldings

Introduction

Whenever currents pass across cell membranes, the existence of differences in the transport numbers of ions (i.e. the fractions of current carried by ions) between membranes and the adjacent solutions, will produce local changes in concentration adjacent to the membranes, which will result in various electrical and osmotic effects. The only uncertainty in any biological situation is the magnitude of the effect. It has already been shown that, in the presence of applied electrical currents, transport number effects can give rise to significant slow changes in the voltage response (and hence in 'apparent membrane conductance'), very large changes in 'apparent membrane capacitance' and significant local osmotic water flows across membranes. These effects have been predicted and demonstrated in *unstirred layers* adjacent to cylindrical plant cells and planar segments of cell walls (Barry & Hope, 1969*a*,*b*); planar sheets of epithelia (Wedner & Diamond, 1969; Noyes & Rehm, 1971) or reconstituted lipid membranes (Smith, 1977) and ion-exchange membranes (e.g. Dewhurst, 1960; Lakshminarayanaiah, 1967; Segal, 1967; Neher & Lux, 1973; MacDonald, 1976). For details, *see* recent reviews (Barry, 1983; Barry & Diamond, 1984). Other examples of ion depletion and enhancement effects during electrical activity near membranes of nerve and muscle cells have been considered in a symposium (Orkand, Nicholson, Ortiz, Almers, Morad, and Eisenberg *in* Orkand, 1980).

It has been shown that the large, slow decrease in conductance measured in response to small-to-medium hyperpolarizing current or voltage pulses (magnitude $\lesssim$ 30 mV) in skeletal muscle fibers is also due to transport number effects (Almers, 1972; Barry & Adrian, 1973). In this case the transport number effects result in a decrease in K^+ concentration within the transverse tubular system (TTS) of muscle, which acts as an *unstirred region* with a relatively large membrane area and small volume within the muscle. In addition to the time-dependent decrease in conductance in response to con-

stant current or voltage pulses, these effects should also give rise to a very large 'apparent capacitance' in muscle in response to sinusoidal currents at very low frequencies (e.g. 24 to 28 $\mu F \cdot cm^{-2}$ at 0.01 Hz; Barry, 1977). This would help to explain some of the discrepancies between experimental and predicted values of skeletal muscle impedance observed in the 1 to 10 Hz range by other workers (Valdiosera, Clausen & Eisenberg, 1974).

Many cell membranes are highly invaginated, particularly, for example, membranes of many neurones such as those of a nudibranch mollusc (Mirolli & Talbott, 1972) or of *Aplysia* (Coggeshall, 1967; Graubard, 1975). The invaginations are similar to the TTS of skeletal muscle in that they provide unstirred regions of relatively large surface area and small volume. These cells are also known to exhibit slow potential changes during long current pulses and it is therefore of value to model the local changes in concentration, and hence the slow potential changes that would be expected to take place as a result of transport number effects under these conditions.

Such transport number effects have been postulated for K^+ accumulation in membrane invaginations of the R_{15} cell of *Aplysia,* to account for slow potential changes in that cell during long depolarizing current pulses (Eaton, 1972). As expected from such a mechanism, Eaton was able to show experimentally that either increasing the external concentration of K^+ or adding tetraethylammonium (TEA) to block potassium conductance reduced these slow potential changes, bringing the steady-state voltage changes close to the 'instantaneous' values. There also seemed to be some correlation between the degree of invagination, as observed morphologically, and the magnitude of the potential changes.

It may readily be seen that dendrites are exactly equivalent to reversed invaginations. They will be especially important in cells with low concentrations of permeant ions. One possible candidate would be calcium, which is at a very low concentration (10^{-7} to 10^{-8} M, e.g. Kostyuk, 1981) within cells and yet which can in some circumstances carry a significant fraction of the membrane current. For example, an inward current would increase internal calcium. This could reduce the currents by either reducing the driving force on calcium or directly reducing the calcium conductance and may thus help to explain the slow 'inactivation' properties of such calcium currents observed in some circumstances, which are less pronounced in situations in which calcium is buffered and held low by a calcium chelating agent (*cf.* Tsien, 1983).

Although neuronal examples of invaginated membranes most readily come to mind, this present treatment should be equally applicable to any invaginated epithelial cells or perhaps even to concentration changes within the lateral intercellular spaces between epithelial cells.

The aim of this paper has been to model such transport number effects as a function of nondimensional membrane parameters, so that when these parameters are estimated, the magnitudes and time course of the voltage changes can easily be calculated. Because of the more general nature of the approach and the greater ease of analysis, the effects will be modeled for a planar invaginated membrane. The results should be readily applicable to cells of any shape and to concentration changes in either invaginations or dendrites. In addition to the main model presented in this paper, which pertains to transport number effects occurring within membrane invaginations, the role of three other transport number situations will also be discussed and the relative magnitude of their contributions assessed and compared with transport number effects within invaginations. These other transport number effects relate to: (1) changes in the average concentration of the ions within the cell interior; (2) changes in the average concentration of the ions within a restricted diffusion region surrounding a cell and (3) changes in the interface concentration of the ions in an unstirred region surrounding a cell.

Principles Underlying Transport Number Effects

The transport number effect (*see* Barry & Hope, 1969*a*; Barry & Adrian, 1973; and also Dewhurst, 1960) is illustrated in Fig. 1*A*. The basic principles can be most readily appreciated by considering the following example in which a cation-permeable membrane separates two solutions containing only K^+ and Cl^-. In the two KCl solutions shown, the transport numbers t_K and t_{Cl} (representing the fraction of current carried by each ion are given, respectively, by $u_K C_K/(u_K C_K + u_{Cl} C_{Cl})$ and $u_{Cl} C_{Cl}/(u_K C_K + u_{Cl} C_{Cl})$ where u and C refer to mobility and concentration, and subscripts K and Cl to K^+ and Cl^- ions, respectively) for both K^+ and Cl^- will be approximately 0.5. In the cation-permeable membrane, however, t_K will be approximately 1.0 and t_{Cl} will be approximately zero. This means that whenever a current is passed across the membrane, for example from right to left in Fig. 1*A*, there will be an equal loss of both K^+ and Cl^- ions in the solution at the right side of the membrane. The rate of loss or gain of KCl, Φ_{KCl}, for a current of i A $\cdot$ cm^{-2}, will be given (Barry & Adrian, 1973) in mol $\cdot$ $cm^{-2} \cdot sec^{-1}$ by

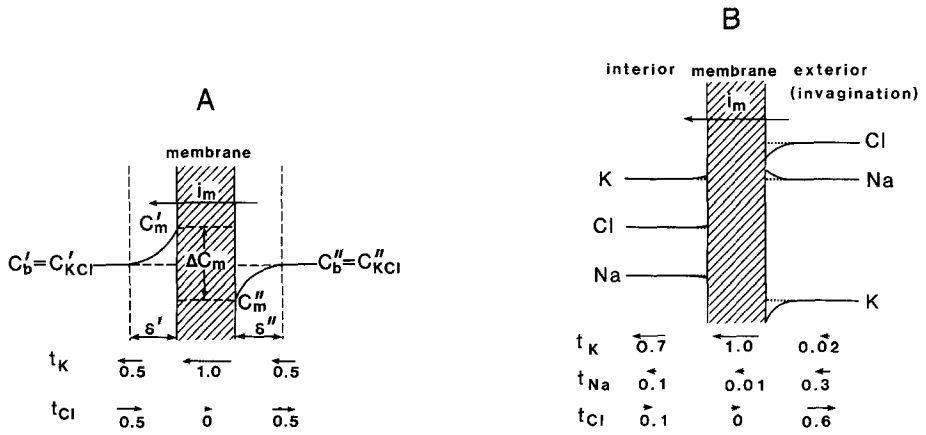

Fig. 1. Panel *A* is a schematic diagram illustrating the transport number effect for a simple cation-selective membrane separating two equal KCl solutions, somewhat similar to Fig. 1 of Barry and Hope (1969*a*) and Fig. 23 of Barry and Diamond (1984). t_K and t_{Cl} represent the transport numbers of K^+ and Cl^- ions, respectively, the magnitude and direction of their contribution to the current i_m being indicated by the length and orientation of the arrows. These transport number discrepancies at each membrane-solution interface give rise to KCl depletion and enhancement in unstirred layers δ'' and δ' in the solutions on each side of the membrane. C_b and C_m represent the KCl concentrations in the bulk solution (assumed to be perfectly stirred for the ideal case) and at the solution side of the mixture-solution interface. This effect gives rise to a concentration difference of electrolyte across the membrane ΔC_m which results in a time-dependent potential difference and the possibility of a local osmotic waterflow (*not shown*). Such concentration effects will be opposed by solute diffusion between this region and the bulk solution. Panel *B* represents the transport number effect for a cell within an invaginated membrane system. Using relative ionic concentrations, which are somewhat representative of a neurone (actually obtained from squid axon data; Bullock, Orkand & Grinell, 1977, p. 132, with mobilities from Robinson & Stokes, 1965) transport numbers for the three major permeant ions K^+, Na^+ and Cl^- were estimated to have the values (rounded-off to the accuracy shown) indicated below each of the three compartments—the interior solution, the membrane itself and the exterior solution together with any invaginated regions. On each side of the membrane the relative concentration changes should be approximately as indicated—the magnitude of the changes within the invaginated region being much greater than in the interior solution. It may readily be seen that for an inward current i_m, as shown, in response to a hyperpolarizing pulse there will be a drop in K^+ within any invaginated region, which will be paralleled by both a drop in Cl^- and an increase in Na^+. In this example, the relative changes in K^+ will be greater than for Na^+ and Cl^- and these changes will be in such a direction as to reduce the driving force on the K^+ ions (*see also* Fig. 2)

$$\Phi_{KCl} = \frac{(t_K^m - t_K^s)i}{F} = -\frac{(t_{Cl}^m - t_{Cl}^s)i}{F} \qquad (1)$$

where superscripts m and s refer to the membrane and solutions, respectively, and where F is the Faraday. It should be noted that Eq. (1) automatically preserves electroneutrality and that the loss or gain in KCl will tend to be balanced primarily by diffusion within the unstirred layers (to or from the bulk solution)[1]. This perturbation of the local salt concentrations on either side of the membrane will give rise to a diffusion potential which will slowly increase to a maximum during the passage of current across the membrane. This time-dependent increase in membrane potential, in the same direction as the *IR* voltage jump, will masquerade as a time-dependent increase in membrane resistance and as a capacitance. The local salt gradient across the membrane will also result in a local osmotic volume flow, which may be mistaken for electro-osmosis, were it not for the relatively slow onset of these transport number effects under most conditions (Barry & Diamond, 1984). When the concentrations of perturbed electrolyte are different on both sides of a membrane, the relative changes in concentration will be greatest at the low concentration side and for large currents will be significantly greater when there is *depletion* rather then *enhancement* of salt at that side.

In a more typical biological case, for a cell with a low anion permeability and an ion distribution similar to that seen in neurones and axons, the transport number changes will be as illustrated in Fig. 1*B*. In the external solution, which normally has a low K^+ concentration the current will mainly

[1] In the case of a fairly 'leaky' membrane (e.g. an ion-exchange membrane with significant external salt concentrations) it may also be significantly balanced by back-diffusion of KCl across the membrane. This could occur even though $t_K^m \gg t_{Cl}^m$, if the membrane's solute permeability P_{KCl} is significant in comparison with $\delta \cdot D_{KCl}$, where δ is the unstirred layer thickness (*see* Barry & Hope, 1969*a*). For most biological cell membranes back-diffusion may generally be neglected.

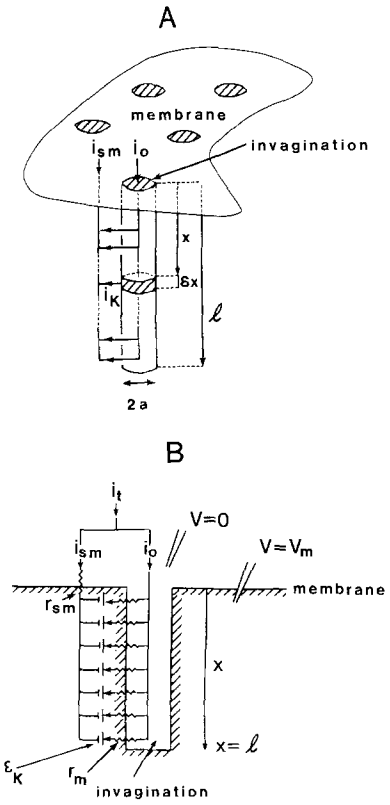

Fig. 2. Panel *A* is a schematic diagram of an invaginated membrane, somewhat similar to Fig. 29 of Barry and Diamond (1984). It shows an area of surface membrane with a number of invaginations (normal or reversed-dendrites), which are assumed for simplicity to be cylinders of length ℓ and radius a. Current i_t (as indicated in Panel *B*) is divided between that going through each invagination i_o and that going through the surface membrane i_{sm}. i_o is then distributed along the length of the invagination as indicated, the current density i_K entering the cell across a region of the invagination δx at distance x is considered to be primarily carried by K^+. Panel *B* is a schematic diagram of the electrical circuit of Panel *A* illustrating the current distribution between the surface membrane resistance r_{sm} and the membrane resistance r_m across the wall of the invagination. The emf's ε_K shown are meant to represent the change in K^+ equilibrium potential, for example, due to K^+ depletion in the invagination during hyperpolarizing pulses, which will oppose the driving voltage so reducing the driving force producing the current i_K

be carried by both Na^+ and Cl^-. In the membrane, the current will primarily be carried by K^+ and within the cell, because of the presence of a high concentration of large immobile or impermeable organic anions, the current will tend to be carried mainly by K^+ and to a small extent by Cl^- and Na^+. The concentration changes, again balanced primarily by diffusion will be as shown in Fig. 1*B*. Since membrane potentials are normally mainly determined by the major permeant ions, the main ionic concentration change that needs to be considered is the K^+ concentration change at the external membrane-solution interface.

Furthermore, these changes in salt gradient and resulting diffusion potential components will always be in the direction opposite to the applied voltage, so that even in a planar membrane system, this will reduce the driving force and hence the magnitude of the current across the membrane. For a nonuniform membrane system, such as an invaginated membrane, the membrane current density will become least where transport number concentration changes are maximal. For constant current pulses, especially, this results in a redistribution of the current from these regions to those with the smallest concentration changes. This means that the effective area over which current is flowing has been reduced, thereby increasing the overall resistance.

Description of the Model

For simplicity it will be assumed that an invaginated cell membrane can be treated as a planar sheet with invaginations that can be approximated as cylinders, but which need not be straight. Obviously, the planar sheet analysis is, in principle, equally applicable to dendrites, which are simply reversed invaginations. However, if there is a large number of dendrites in a small cell, the finite size of the unstirred interior compartment will mean that the following analysis will underestimate the magnitude of the concentration changes and hence potential changes. The model will be assumed to be as illustrated in Fig. 2*A* with the electrical circuit as shown in Fig. 2*B*. Since the most significant local concentration change will occur within the invaginations, the analysis is applicable to a membrane of any shape, provided that the membrane space constant is long in comparison with the dimensions of the cell and that the external solution is approximately equipotential. On the other hand, it will apply to a spherical cell of any size provided that the internal electrodes are reasonably centrally placed within the cell. In addition, there is no loss in generality in considering cylindrical invaginations, provided that the diameter of the invagination is small in comparison with its length. The model will therefore be applicable to a biological cell membrane with tortuous invaginations.

The resulting changes in membrane potential and apparent conductance will be calculated for constant current pulses. In principle, the analysis can be readily modified to investigate the response to constant voltage pulses, or to a sinusoidal current, for low-frequency impedance analysis.

The basic principles of the effect are as follows.

If a constant current i_t is applied across the cell membrane, some of the current i_{sm} crosses the surface membrane while the rest i_o goes across the membrane of the invaginations. Because of the relatively larger area of the invaginated membrane region, it will generally make the major contribution to the membrane conductance. Provided that the invaginations have homogeneous membrane properties, a reasonably low luminal resistance and a uniform ionic composition within them at the onset of the current pulse, the current density should be initially constant along the length of the invagination. After a short time, the transport number effects would result in a change in local ionic concentration within the invaginations. These concentration changes would be opposed primarily by diffusion into (out of) the invaginations when the ion concentrations are being depleted (enhanced) there. The concentration changes would be maximal at the closed-end of the invaginations and minimal at the open-end. As already mentioned, these concentration changes are in the opposite direction to the applied voltage, and hence will maximally reduce the driving force and membrane current deep within the invaginations. In the constant current situation, this will force more current across that part of the invaginated membranes near their open-ends and across the surface membrane itself, whereas in the constant voltage case it will simply decrease the overall current.

Both analytical and numerical analyses will be undertaken. In each case it will be assumed that over the range of driving forces considered, the membrane conductance is constant and independent of driving force.

In order to simplify the equations for the time-dependent analytical treatment two further assumptions will be made: (1) that the luminal resistance of the invaginations is small so that the potential drop within the lumen is small and (2) that the relative concentration changes $\Delta C/C$ are not too large so that $\log_e(1 \pm \Delta C/C) \cong \pm \Delta C/C$.

For the analytical steady-state treatment the first assumption above can be relaxed and for the numerical analysis neither assumption is required.

Theory

A planar membrane region of the type shown in Fig. 2*A* will be assumed in which there are n cylindrical invaginations of length ℓ cm and radius a cm per cm^2 of surface membrane. The following treatment is also equally applicable with minor modification (*see* footnote 3) to wide, thin membrane invaginations or infoldings. In both cases, a total hyperpolarizing current i_t across 1 cm^2 of surface area of a cell, will have two components: i_{sm}, the current density, across the surface membrane and ni_o, the sum of all the currents going down the n invaginations. For simplicity at this stage, it will be assumed that the membrane is uniform so that

$$G_{sm} = G_m = 1/R_m \tag{2}$$

where G_{sm} and G_m are the ionic conductances of 1 cm^2 of surface and invaginated membranes, respectively, and R_m the resistance of 1 cm^2 of membrane. For purposes of discussion it will be assumed that the major permeant ion is K^+, but it should be realized that the principles apply also to any other major permeant ion, particularly if it also has a low absolute concentration within the invagination or dendrite. From the above

$$i_t = i_{sm} + ni_o. \tag{3}$$

Within a volume element of thickness δx and down an invagination at a distance x from the surface, the potassium current density i_K across the membrane of the invagination will cause a decrease in concentration $C = C(x)$ of K^+. This will be opposed by diffusion and is given by

$$\frac{\partial C}{\partial t} = -\frac{2i_K}{aF} + D\frac{\partial^2 C}{\partial x^2} \tag{4}$$

where $t^m - t^s$, the transport number difference between the lumen of the invagination and its membrane has been approximated as 1.0 (*cp.* Fig. 1*B*), F is the Faraday and D is the diffusion coefficient of the ion (in this case K^+) partially diffusing with Cl^- and partially exchanging with Na^+ along the lumen of the invagination. The K^+ current density i_K at distance x can be related to the driving force on K and hence to both the voltage across the invagination and the potassium concentration gradient by

$$i_K = -G_m\left(\Delta V_m - V(x) - \frac{RT}{F}\ln\frac{C(x)}{C_o}\right) \tag{5}$$

where C_o is the concentration of K^+ initially within the invaginations and in the external solution throughout the time course of the pulse. ΔV_m represents the *change* in membrane potential from the resting potential and $V(x)$ the potential within the invagination (with respect to the external solution), just as $(RT/F)\ln C(x)/C_o$ represents the *change* in the potassium equilibrium potential. The potential drop down the lumen of the invaginations will be given by

$$\frac{\partial V}{\partial x} = -i(x)/(\pi a^2 G_L) \tag{6}$$

where $i(x)$ is the current down an invagination at distance x and G_L is the luminal conductivity. If G_L is large enough then $\partial V/\partial x \cong 0$ and the lumen may be considered to be approximately isopotential.

In addition, provided $[C(x) - (C_o)]/C_o \ll 1$ then Eq. (5) may be linearized to

$$i_K \cong -G_m \left[\Delta V_m - V(x) + \frac{RT}{F}\left(1 - \frac{C}{C_o}\right)\right]. \tag{7}$$

The error resulting from this approximation will be maximal down the invagination where $[\Delta V_m - V(x)]F/RT$ may eventually approach $\Delta C/C_o$. In fact, generally $|\Delta C/C_o| \lesssim |\Delta V_m F/RT|$. For example, if $\Delta V_m \cong 1$ mV then $|\Delta C/C_o| < 0.04$. A value of 0.040 for $\Delta C/C_o$ results in $|\log[(C - \Delta C)/C_o]| \cong 0.0408$, indicating only a 2% error for the current in that part of the invagination. This has been quantitatively checked by comparison with the numerical analysis values (*see* Numerical Analysis section for further details) and is illustrated in Fig.7 for three different amplitude currents. For $\Delta V_m = 1$ mV the actual error in the voltage ΔV_m is only 1.4% (compare curves *b* & *c* of Fig. 7).

Within the limits of this linear approximation, a symmetrical response will be predicted for depolarizing and hyperpolarizing currents, with a corresponding depletion or enhancement of K^+ within the invaginations. From the principle of charge conservation along the invagination, we also have that

$$i_K = -\frac{1}{2\pi a}\frac{\partial i}{\partial x} \tag{8}$$

where i is the longitudinal current flowing down the invagination at distance x. Hence, integrating all along the length of the invagination, the total current entering it will be given by

$$i_o = 2\pi a \int_0^\ell i_K dx. \tag{9}$$

In addition, the boundary conditions are

(i) $C = C_o$ at $x = 0$ for all t.

(ii) $C = C_o$ for all x when $t = 0$.

(iii) $\partial C/\partial x = 0$ at $x = \ell$.

Condition (i) represents the fact that the invagination with its small volume opens out suddenly into a much larger volume, so that to a first approximation this external volume will behave as a perfectly stirred solution reservoir[2]. For a large number of invaginations, and especially dendrites in a small cell, this assumption will tend to cause an underestimate of the magnitude of these transport number effects. Condition (ii) assumes that there has been enough time between current pulses for the concentration of K^+ within the invagination to relax to its initial uniform value which is the same as that in the external solution. Condition (iii) reflects the internal end of the invaginations being closed.

Time-Dependent Solution (with Infinite Luminal Conductivity)

In order to solve the time-dependent equations it will be assumed that the conductivity of the lumen of the invaginations is high enough so that they may be considered to be equipotential. As will be shown in the next section this is a reasonable assumption for physiological solutions provided transport number effects are not too great.

The total current i_t entering the cell is given by

$$i_t = ni_o - \Delta V_m/R_m. \tag{10}$$

It will be shown in Appendix A that the solution to these equations in dimensionless units, giving the relative change in membrane potential due to transport number effects, is given by

$$\begin{aligned}\Delta V(T')/\Delta V(0) &= -\Delta V_m/IR_m^* \\ &= (1 + \delta A)[A_1(\beta) + A_2(\alpha,\beta)e^{-(\alpha^2-\beta)T'} \\ &\quad + \sum_{m=1}^{\infty} A_2(i\alpha_m,\beta)e^{-(\alpha_m^2+\beta)T'}]\end{aligned} \tag{11}$$

where R_m^* the combined membrane resistance of the surface and the invaginations for 1 cm^2 of surface is related to R_m and G_m by

$$R_m^* = \frac{R_m}{1 + \delta A} = \frac{1}{G_m(1 + \delta A)} \tag{12}$$

and where T' is the time in dimensionless units related to real time t by

$$T' = Dt/\ell^2. \tag{13}$$

$A_1(\beta)$ is given by

[2] An access resistance condition can be incorporated into these equations by changing condition (i) to $\partial C/\partial x = h(C(0) - C_o)$ where $C(0)$ is the concentration just within the invagination at $x = 0$ and $V(0) = i_o n r_s$ where r_s is the total access resistance per cm^2 of surface membrane and $h = 1/(n\pi a^2 r_s G_L)$ where G_L is the conductivity of the lumen of the invaginations.

$$A_1(\beta) \equiv \frac{1}{1 + \delta A\ (\tanh \sqrt{\beta})/\sqrt{\beta}} \tag{14}$$

where the transport number parameter β is defined by[3]

$$\beta \equiv 2G_m RT\ell^2/(aF^2C_oD). \tag{15}$$

δA, representing the area of the invaginated membrane for 1 cm^2 of surface membrane, is given by[3]

$$\delta A = 2\pi na\ell. \tag{16}$$

$A_2(\alpha,\beta)$ is given by:

$$A_2(\alpha,\beta) \equiv \frac{\alpha^2}{(\alpha^2 - \beta)[Z_1(\alpha) + Z_2(\alpha)\tanh \alpha]} \tag{17}$$

where the value of α is given by the root (if it exists) of

$$\alpha^2 + \delta A\left[\alpha^2 + \beta\left(\frac{\tanh \alpha}{\alpha} - 1\right)\right] = 0 \tag{18}$$

with the condition that $\alpha^2 < \beta$.

$$Z_1(\alpha) \equiv 1 + \delta A + \frac{\delta A \cdot \beta}{2\alpha^2} \tag{19}$$

$$Z_2(\alpha) \equiv \frac{\alpha}{2}(1 + \delta A) - \frac{\delta A \cdot \beta}{2\alpha^3}(\alpha^2 + 1). \tag{20}$$

Similarly, for each value of m, $A_2(i\alpha_m,\beta)$ is given by

$$A_2(i\alpha_m,\beta) \equiv \frac{\alpha_m^2}{(\alpha_m^2 + \beta)[Z_1(i\alpha_m) + iZ_2(i\alpha_m)\tan \alpha_m]} \tag{21}$$

where the α_m are the roots of

$$\alpha_m^2 + \delta A\left[\alpha_m^2 - \beta\left(\frac{\tan \alpha_m}{\alpha_m} - 1\right)\right] = 0 \tag{22}$$

and where with $i = \sqrt{-1}$, $Z_1(i\alpha_m)$ and $iZ_2(i\alpha_m)$ are defined as

$$Z_1(i\alpha_m) \equiv 1 + \delta A - \frac{\delta A \cdot \beta}{2\alpha_m^2} \tag{23}$$

and

$$iZ_2(i\alpha_m) \equiv -\frac{\alpha_m}{2}(1 + \delta A) + \frac{\delta A \cdot \beta}{2\alpha_m^3}(1 - \alpha_m^2). \tag{24}$$

For large values of m it may be shown that $\alpha_m \cong m\pi/2$. When $T' \to \infty$ the steady-state value of $\Delta V_m/IR_m^*$, $\Delta V(\infty)/\Delta V(0)$, is given from Eqs. (11) and (14) by

$$\frac{\Delta V(\infty)}{\Delta V(0)} = \frac{\Delta V_m}{IR_m^*} = -\frac{\Delta V_m(1 + \delta A)}{IR_m} = \frac{1 + \delta A}{1 + \delta A(\tanh \sqrt{\beta})/\sqrt{\beta}}. \tag{25}$$

As a check that no α or α_1 roots had been missed, and that there has been no error in the analytical equations derived in Appendix A (*see also* discussion in section on Numerical Analysis and Appendix C), $\Delta V_m/IR_m^*$ can be calculated for $T' = 0$, in which case $-\Delta V_m/IR_m^* = 1$ so that

$$(1 + \delta A)\left[A_1(\beta) + A_2(\alpha,\beta) + \sum_{m=1}^{\infty} A_2(i\alpha_m,\beta)\right] = 1.0. \tag{26}$$

In the calculations used for this paper this was normally satisfied to well within 1 part in 10^5, even when the steady-state value of $-\Delta V_m/IR_m^*$ was greater than 30. The root of Eq. (18) was obtained using a combination of a traversing technique and Newton's method, whereas the roots of Eq. (22) were obtained using Newton's method alone. Analytical calculations were all done in double precision using Fortran IV on an LSI-11 microprocessor (Digital Equipment Corporation, Maynard, Massachusetts).

Steady-State Solutions (Finite Luminal Conductivity)

For the general finite luminal conductivity case, which is analyzed in terms of nondimensional parameters in Appendix B, the voltage drop down the invaginations dV/dX will be given by Eqs. (B3), (B7) and (B9). The final voltage response $\Delta V(\infty)/\Delta V(0)$ may be given [Eq. (B26)] by

$$\frac{\Delta V(\infty)}{\Delta V(0)} = \frac{1 + \delta A(\tanh \sqrt{\beta\Theta})/\sqrt{\beta\Theta}}{1 + \delta A(\tanh \sqrt{\beta'})/\sqrt{\beta'}} \tag{27}$$

where β' is defined by

[3] For wide thin membrane invaginations or infoldings (width w, thickness d and length ℓ, where $d \ll w$) the treatment is identical except that then $2\pi a$ should be replaced by wd and $a/2$ by d in the equations so that $\beta \cong G_m RT\ \ell^2/(dF^2C_oD)$ and $\delta A \cong nwd\ell$.

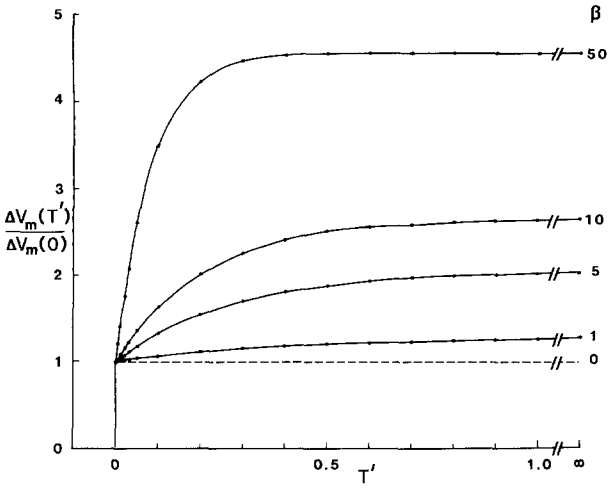

Fig. 3. The time-dependent slow potential changes, caused by transport number depletion or enhancement of ions (e.g. K^+) within invaginated regions of a membrane, during constant current pulses and calculated using the analytical equations. $\Delta V_m(T')/\Delta V_m(0)$ represents the increase in the membrane potential after time T' expressed in nondimensional units relative to its instantaneous (neglecting true capacitance transients) value. The nondimensional time T' may be converted to real time using the relationship $t = \ell^2 T'/D$ [Eq. (32)]. The values shown were calculated using Eqs. (11)–(25) for a relative area of invaginations δA [Eq. (16)] of 10 and for various values of the nondimensional transport number β [*see* Eq. (15)] as indicated. The dashed line (equivalent to $\beta = 0$) represents the voltage response in the absence of transport number effects. Note the increase in response with β and the decrease in the time to reach steady state (shown more clearly in Fig. 4)

$$\beta' \equiv \beta(1 + \Theta) \tag{28}$$

and Θ and $\beta\Theta$ by

$$\Theta = DF^2C_0/RTG_L \tag{29a}$$

$$\beta\Theta = 2G_m\ell^2/aG_L. \tag{29b}$$

For small values of Θ, $\beta' \to \beta$ and $\tanh \sqrt{\beta\Theta}/\sqrt{\beta\Theta} \to 1$ and Eq. (27) reduces to Eq. (25). Larger values of Θ in part serve to increase the magnitude of the effective transport number parameter. For typical values of physiological solutions ($D = 1.5 \times 10^{-5}$ $cm^2 \cdot sec^{-1}$, $C_o = 5 \times 10^{-6}$ $mol \cdot cm^{-3}$, $G_L = 10^{-2}$ $S \cdot cm^{-1}$) $\Theta \cong 0.03$ and represents a 3% correction to β. As may be noted from inspection of Eq. (29a) although Θ is independent of invagination geometry $\beta\Theta$ is not and increases as β increases. For $\beta = 10$ and $\Theta = 0.03$, $(\tanh \sqrt{\beta\Theta})/\sqrt{\beta\Theta} = 1.088$, which results in an overall correction of about 8–9%.

Numerical Analysis

In order to produce an exact solution of these transport number equations, which would justify (and determine the limitations of) the linear logarithmic approximation and would further readily allow an investigation of the response at the end of a current pulse, a numerical analysis was undertaken as outlined in Appendix C. For comparison with the linear logarithm approximation [Eq. (7)] the numerical analysis gave results which were well within 0.05% of the analytical values (using 50 elements and a 0.0002 time step).

The numerical analysis is readily able to handle both the current-on and current-off voltage responses. In the case of the linear logarithm approximation it can easily be shown that the on and off responses are exactly symmetrical (e.g. Fig. 7). In other words describing the on response at any time T' after the beginning of the current pulse [*see* Eqs. (11–26)] by

$$\frac{\Delta V(T')}{\Delta V(0)} = 1.0 + F(\infty)[1 - f(T')]. \tag{30}$$

The off response is then simply

$$\frac{\Delta V(T' + T'')}{\Delta V(0)} = F(\infty)f(T'') \tag{31}$$

where $f(0) = 1$ and $f(\infty) = 0$, $F(\infty)$ is the steady-state magnitude of the transport number contribution and T'' represents the time after the turn-off of a long current pulse of length T'. In both equations $\Delta V(0)$ represents the voltage response at the beginning of the current pulse. The numerical analysis also indicated the magnitude of the deviation of the voltage response when the exact logarithm expression is used for different values of $\Delta V(0)F/RT$ and this is shown in Fig. 7.

Theoretical Predictions

In order to make the analysis as general as possible, the equations and predicted figures have all been calculated using dimensionless parameters. In order to assess a particular response, the relative area of the invaginations and the transport number parameter need to be evaluated from Eqs. (16) and (15). The half-time $T'_{1/2}$ and the general time parameter T' may then simply be transformed to real time t values using

$$t = \ell^2 T'/D \tag{32}$$

and

$$t_{1/2} = \ell^2 T'_{1/2}/D. \tag{33}$$

Figure 3 shows the voltage response $\Delta V_m(T')/\Delta V_m(0)$ ($\equiv -\Delta V_m/IR^*_m$ in Eq. (11)) for a constant

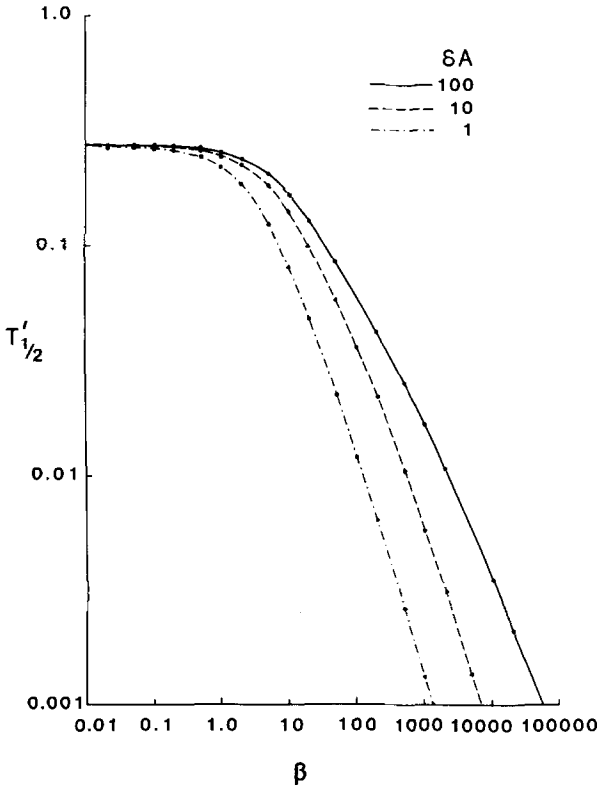

Fig. 4. The half-time $T'_{1/2}$ in nondimensional units for the slow potential changes, caused by transport number depletion or enhancement of ions within invaginated regions of a membrane, during constant current pulses calculated using the analytical equations. This is shown for three different relative areas of invagination δA (Eq. (16)) as a function of the nondimensional transport number parameter β [Eq. (15)]. The nondimensional half-time $T'_{1/2}$ may be converted to a real half-time $t_{1/2}$ by using the relationship $t_{1/2} = \ell^2 T'_{1/2}/D$ [Eq. (33)]. It may be seen that $T'_{1/2}$ asymptotes to a value of about 0.27 for very small values of β (close to the value of $4/\pi^2 \ln 2 \cong 0.28$ calculated from the time constant due to the first root of Eq. (22) alone for small values of β). Note also that $T'_{1/2}$ decreases very rapidly with β for values greater than about 5.0. $T'_{1/2}$ was calculated numerically by determining the value of T' at which $(\Delta V_m(T') - 1)/(\Delta V_m(\infty) - 1) = 0.5$. As discussed in the text and Fig. 7 these analytical values will only significantly overestimate $T'_{1/2}$ for very large currents

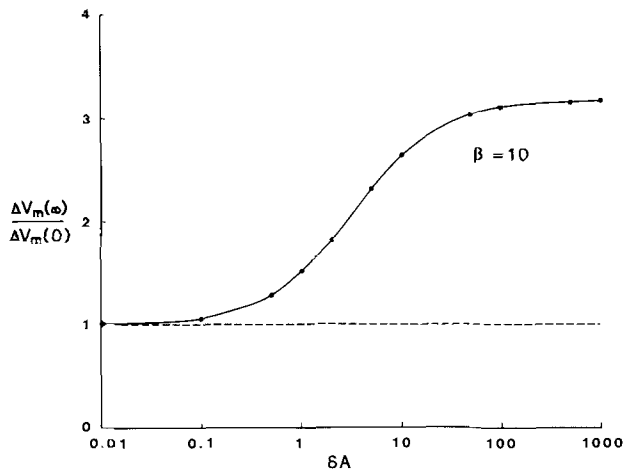

Fig. 5. The steady-state amplitude of the slow potential changes caused by transport number depletion or enhancement of ions within membrane invaginations during constant current pulses and calculated using the analytical equations. $\Delta V_m(\infty)/\Delta V_m(0)$ represents the increase in membrane response at infinite time ($T' = \infty$) relative to its instantaneous value ($T' = 0$). The instantaneous value is the same as that in the absence of transport number effects ($\beta = 0$). This is shown for a nondimensional transport number parameter β (Eq. (15)) of 10 as a function of the relative area of the invaginations δA (Eq. (16)). Note that as δA increases above 100, the amplitude of the slow voltage response saturates

current pulse in the presence of transport number effects after time T', relative to its value at zero time before transport number effects could increase the magnitude of the voltage response. These results are shown as a function of transport number parameter β for a value of $\delta A = 10$. It may be seen that this slow voltage response rises to a maximum steady-state level which increases with the magnitude of β, a value of $\beta = 0$ being equivalent to no transport number effects or perfectly stirred invaginations. It may be seen that the voltage response for $T' = 1$ is hardly distinguishable from the infinite value. Furthermore the half-time for the response which is determined to a very good approximation by the first time constant [i.e. $T'_{1/2} \sim 0.693\tau$, where $\tau \sim 1/(\alpha^2 - \beta)$ (if α exists) or $1/(\alpha_1^2 + \beta)$ (if α does not exist)] in Eq. (11) is seen to decrease as β increases. This is shown more clearly in Fig. 4 where $T'_{1/2}$ has been obtained numerically from Eq. (11) for different values of β and three different values of δA. Note that for $\beta < 0.5$ and $\delta A > 10$, $T'_{1/2} \cong 0.27$. However, as β increases much beyond 2, $T'_{1/2}$ begins to decrease radically. $T'_{1/2}$ however, increases slightly in this region as δA increases.

Figure 5 shows the steady-state voltage response compared to its instantaneous value ($T' = 0$). This instantaneous value is identical to the response in the absence of transport number effects (i.e. $\beta = 0$) as indicated in Fig. 6. From Eq. (11)

$$\frac{\Delta V_m(\infty)}{\Delta V_m(0)} = (1 + \delta A)A_1(\beta). \tag{34}$$

For very large values of δA ($\delta A \to \infty$), the relative area of the membrane invagination, substituting for $A_1(\beta)$ from Eq. (14)

$$\frac{\Delta V_m(\infty)}{\Delta V_m(0)} \cong \sqrt{\beta} \coth \sqrt{\beta} \tag{35}$$

so for a value of $\beta = 10$, as in Fig. 5, this asymptotes to a saturating value of approximately 3.17.

Actually for $\beta > 10$,

$$\Delta V_m(\infty)/\Delta V_m(0) \cong \sqrt{\beta}. \tag{36}$$

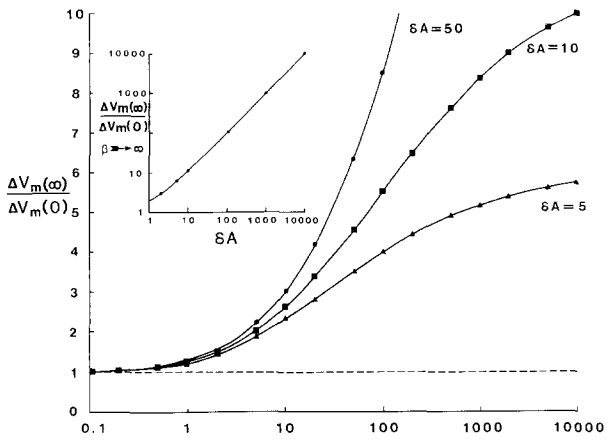

Fig. 6. The main panel shows the steady-state amplitude of the slow potential changes as $\Delta V_m(\infty)/\Delta V_m(0)$, as depicted in Fig. 5, as a function of transport number parameter β for various values of relative invagination area δA and calculated using the analytical equations. Note that for a fixed value of δA it saturates for large values of β, the level to which it saturates increasing with δA. The inset shows that as for very large values of β ($\beta \to \infty$), the magnitude of the slow voltage response continues to increase with δA

For a fixed value of δA the voltage response also asymptotes as β is increased, as shown in Fig. 6. For very large values of β ($\beta \to \infty$)

$$\frac{\Delta V_m(\infty)}{\Delta V_m(0)} \cong 1 + \delta A \tag{37}$$

as indicated in the inset to Fig. 6.

Figure 7 shows both the current-on and current-off voltage responses, calculated using the full numerical analysis. For the two linear approximations (or for low current values) the current-on and current-off responses are exactly symmetrical [*see* Eqs. (30) & (31) and curves *b* and *d* in Fig. 7]. For larger values of current, using the exact logarithm expression, the symmetry of the two responses is not so precise. In addition, larger values of current also increase the magnitude of the transport number effects and accelerate its rate of onset. However, this decrease only becomes significant at very large currents. For example, even for $\Delta V_m \cong -20$ mV, $T'_{1/2}$ has only decreased to 0.13 from its zero current value of 0.14, whereas for $\Delta V_m \cong -40$ mV it drops rather more significantly to 0.09. For the very large values of current (e.g. curve *f* in Fig. 7), the permeant ion concentrations within the invagination will be depleted to almost zero. As the analysis stands this will tend to result in an overestimate of both the magnitude and rate of onset of the transport number effects. This will occur because the transport number of the permeant ion in the invaginated membrane will start to decrease when its concentration begins to approach close to zero (i.e. when $\Delta C \to C_0$). For example, from Eq. (5) when $\Delta V_m \cong -20$ mV then the maximum depletion (which will produce zero current) will be given when $\Delta C/C_0 \cong 0.55$ and when $\Delta V_m \cong -40$ mV, $\Delta C/C_0 \cong 0.79$. This dependence of transport number on the absolute concentration of the permeant ion has not been allowed for in the analysis.

Other Transport Number Contributions to Slow Voltage Changes

Transport number effects can contribute to slow time-dependent potential changes, resulting from changes in concentration of the dominant permeant ion, in three additional ways. These are: (1) changes in the average concentration of the ions within the cell interior; (2) changes in the average concentration of the ions within a restricted diffusion region surrounding a cell and (3) changes in the interface concentration of the ions in an unstirred region surrounding a cell. The dependence of these transport number contributions on appropriate membrane and geometric parameters will now be estimated and their relative magnitude compared with those resulting from effects arising in membrane invaginations.

Average Ion Concentration Changes Within Cell Interior

Such ion concentration changes satisfactorily explain the very large and slow potential changes during hyperpolarizing current pulses in mammalian muscle fibers. In this situation, the transport number effects predict and appear to give rise to a very significant depletion of Cl^- within the muscle (Barry & Dulhunty, 1984).

For a small spherical cell of radius r, in which the pulses of duration t seconds are long enough so that diffusional equilibration takes place within the cell interior (i.e. $t \gg r^2/D$) the change in potential δV can be estimated. This can be done, as follows, for the most permeant ion, which will generally contribute most to the membrane potential

$$\delta V \cong \frac{RT}{zF} \ln\left[\frac{C_o}{C_o - \Delta C}\right] \cong \frac{RT\,\Delta C}{zFC_o} \tag{38}$$

where C_0 is the initial internal concentration of the ion and ΔC is its change (e.g. a decrease inside a cell, with a similar equation for an increase outside a cell) after a current pulse of magnitude i with the assumption that $\Delta C/C_o \ll 1$. Now after t seconds

$$\Delta C \cong \frac{\alpha_t it}{zFU} \tag{39}$$

where U is the cell volume and $\alpha_t = t_m - t_e$ is the transport number difference for the particular ion between its value in the membrane and in the current electrode. In this case, if the specific membrane conductance in the absence of transport number effects is G_m (S · cm^{-2}), the applied voltage is ΔV and the cell surface area is A then the current i will be related to ΔV by

$$i = G_m A\ \Delta V. \tag{40}$$

From Eqs. (38) and (39) for a monovalent ion

$$\delta V \cong \frac{RT\alpha_t it}{F^2 UC_o}. \tag{41}$$

Since $U = 4\pi r^3/3$, Eq. (41) can be re-expressed as

$$\delta V \cong \frac{3RT\alpha_t it}{F^2 4\pi r^3 C_o} \tag{42}$$

and hence substituting for i from Eq. (40), since $A = 4\pi r^2$, we obtain the relative increase in potential resulting from transport number effects compared to the potential change in their absence

$$\frac{\delta V}{\Delta V} \cong \frac{3RT\alpha_t G_m t}{F^2 rC_o}. \tag{43}$$

These effects become significant when $\delta V/\Delta V$ approaches or exceeds 1.0. As we have already seen, transport number effects in membrane invaginations also become significant as the transport number parameter for the invaginated membrane β approaches or exceeds 1.0. Therefore for an order-of-magnitude calculation the relative contributions of these two effects R_1 from Eqs. (43) and (15) is given by

$$R_1 = \frac{(\delta V/\Delta V)}{\beta} = \frac{3\alpha_t aDt}{2r\ell^2}. \tag{44}$$

If t is long enough, so that $R_1 \gg 1$, changes in the average internal composition of the cell will produce the most significant contribution, whereas if t is short enough, so that $R_1 \ll 1$, then transport number effects in the membrane invaginations will predominate.

Ion Concentration Changes Within Small Restricted Space Surrounding a Cell

If there is a small restricted diffusional space outside a cell of width d (cm), where $d \ll a$, in which, for a reasonably long current pulse of magnitude i and duration t (seconds), diffusional equilibration generally may be assumed to take place within the space (provided $t \gg d^2/D$) then, for a particular permeant ion, the change in average concentration ΔC within this restricted space would be given by

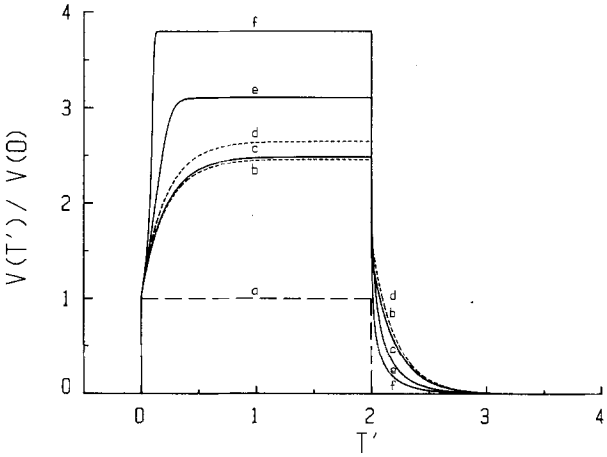

Fig. 7. The time-dependent slow potential changes $V(T')/V(0)$ [equivalent to $\Delta V_m(T')/\Delta V_m(0)$ in the text] caused by transport number effects in invaginated membranes during and following constant current pulses and calculated using the numerical analysis described in the text. Curves (*b–f*) were calculated with a relative invagination area $\delta A = 10$ and transport number parameter $\beta = 10$, using 50 elements and a step size of 0.0002. The dashed rectangular curve (*a*, equivalent to $\beta = 0$) represents the voltage response in the absence of transport number effects. The two dotted curves (*d* and *b*) were calculated using the linear logarithmic approximation of Eq. (7). Curve *d* with $\Theta = 0$ (representing a high conductivity in the lumen of the invaginations) gave identical values (within 0.04%) with those calculated using the analytical treatment for the onset of the current pulse [Eqs. (12)–(25)] and shown in Figs. 3–6. Curve *b* (below curve *d* throughout its time course) was calculated with $\Theta = 0.03$ [*see* Eq. (29a)], to represent typical physiological solution values. The steady-state value for *b*, now somewhat reduced below that in *d*, was again within 0.04% of the analytical value calculated using Eqs. (27)–(29). Computed curves using the linear logarithmic approximation (as in *b* and *d*) were independent of the magnitude of the current. In contrast, curves *c*, *e* and *f*, calculated using the exact logarithmic term [Eq. (5)] were found to be dependent on current magnitude. In each of these cases $\Theta = 0.03$. and curve *c*, with a low magnitude current parameter ($I_t = 0.4$ so that the $\Delta V(0)F/RT \cong 0.04$ and the initial $\Delta V(0) \cong 1$ mV), was very close to curve *b*. However, as I_t was increased to 8 (curve *e*, $\Delta V(0) \cong 20$ mV) and 16 (curve *f*, with $\Delta V(0) \cong 40$ mV) so both the amplitude and the rate of onset (and termination) of the transport number effects was increased. $T'_{1/2}$ however, only decreased from about 0.14 (curve *b*, $I_t = 0.4$) for very small currents to 0.13 (curve *e*, $I_t = 8$), whereas for the very large currents (curve *f*, $I_t = 16$) it decreased to 0.09. Curve *f*, especially, probably overestimates the rate of onset of time-dependent voltage changes since the permeant ion concentration is heavily depleted down to almost zero throughout most of the invagination. Such radical concentration depletion resulting from these high current magnitudes would be likely to reduce both the ion transport number and conductance within the membrane of the invagination, a factor not allowed for in the analysis.

$$\Delta C \cong \frac{\alpha_s it}{zFAd} \tag{45}$$

with

$$\alpha_s \cong t_m - t_s \tag{46}$$

where t_s is the transport number for the ion leaving the space, where A is again the surface area of the cell and the other terms are as previously defined. Again from Eq. (45) and an equation equivalent to Eq. (38), the magnitude of the voltage change δV for a monovalent permeant ion is given by

$$\delta V \cong \frac{RT\alpha_s it}{F^2AdC_o} \tag{47}$$

so that substituting for A

$$\delta V \cong \frac{RT\alpha_s it}{F^2 4\pi r^2 dC_o} \tag{48}$$

and substituting for i from Eq. (40)

$$\frac{\delta V}{\Delta V} = \frac{RT\alpha_s G_m t}{F^2 dC_o} \tag{49}$$

where again G_m is the conductance in the absence of transport number effects. As in the previous case, these effects become significant when $\delta V/\Delta V$, now given by Eq. (49) approaches or exceeds 1.0. Note that the magnitude of the effect is inversely proportional to the thickness of the diffusional space d. Again by comparing $\delta V/\Delta V$ to β, the relative magnitude R_2 of this transport number contribution [Eq. (49)] compared to that within membrane invaginations [Eq. (15)], is given by

$$R_2 = \frac{\delta V/\Delta V}{\beta} = \frac{\alpha_s aDt}{2d\ell^2}. \tag{50}$$

As before, if t is long enough, so that $R_2 \gg 1$, transport number effects within the restricted space will be dominant, whereas if it is short enough, so that $R_2 \ll 1$, the transport number effects within the membrane invaginations will predominate. Also R_2/R_1 from Eqs. (44) and (50) is simply given by

$$R_2/R_1 = \frac{\alpha_s r}{3\alpha_t d}. \tag{51}$$

Concentration Changes in Unstirred-Layer Surrounding Cell

This is the most difficult of the three cases to analyze. Normally it is treated by assuming that beyond an unstirred-layer of thickness δ the solution is perfectly stirred. The transport number and diffusion equations are then solved within this region. This has been done for a planar membrane system (e.g. Barry & Hope, 1969*a*; Barry, 1983; Barry & Diamond, 1984) and the maximum concentration change ΔC in the absence of any negative feedback effects, such as waterflow and solute backdiffusion, is given by

$$\Delta C \cong \frac{\delta\alpha_s \bar{\imath}}{DzF} = \frac{\delta\alpha_s i}{ADzF} \tag{52}$$

where α_s is as defined by Eq. (46) although t_s is now just the transport number within the solution and may differ from the value for an ion leaving a restricted space. Also $\bar{\imath}$ is the current density related to the total current i by

$$i = A\bar{\imath}. \tag{53}$$

Again from Eq. (51) and an equation equivalent to Eq. (38), the magnitude of the voltage change δV for a monovalent permeant ion is given by

$$\delta V \equiv \frac{RT\,\delta\alpha_s i}{F^2 DC_o A}. \tag{54}$$

Using Eq. (40) to express i in terms of G_m and ΔV

$$\frac{\delta V}{\Delta V} \cong \frac{RTG_m\alpha_s\delta}{F^2DC_o}. \tag{55}$$

Note that, in contrast to the previous case, the magnitude of this transport number contribution increases in proportion to the unstirred-layer thickness and, provided that $t \gg \delta^2/D$, is independent of time t. The relative magnitude R_3 of such transport number effects in the external unstirred-layer relative to those occurring within membrane invaginations will be given from Eqs. (52) and (15) by

$$R_3 = \frac{\delta V/\Delta V}{\beta} = \frac{\alpha_s a\delta}{2\ell^2}. \tag{56}$$

Again if $R_3 \gg 1$ this external unstirred-layer transport number contribution will predominate, whereas the membrane invagination contribution will predominate if $R_3 \ll 1$.

It may also be readily seen that the relative contributions of a restricted space of thickness d and an unstirred-layer of thickness δ will simply be given by

$$\frac{R_3}{R_2} = \frac{d\delta}{Dt} \tag{57}$$

where it is assumed that α_s is the same in both cases, D is the diffusion coefficient of the appropriate ion within the unstirred layer and t is the duration of the current pulse.

Biological Relevance

As mentioned earlier, other measurements in some cells do seem to strongly support the hypothesis that membrane invaginations play a significant role in causing slow voltage changes. In order to estimate the magnitude of such transport number effects in a particular cell, it is necessary to know the values of the invagination transport number parameter β [Eq. (15)] and the relative area δA [Eq. (16)] occupied by the invaginations. The magnitude and time course of the effects can then be assessed from Figs. 3–7.

Estimates of 7.5 for the ratio of actual surface area, to that based on a noninvaginated sphere of the same diameter, for the giant neurone of a nudibranch mollusc (Mirolli & Talbott, 1972) and 6 for the ratio of actual soma perimeter to that of a noninvaginated circle of the same diameter for *Aplysia* neurones, together with the range of apparent capacitances from about 3 to 56 $\mu F \cdot cm^{-2}$ (cited in Andrews, 1977), suggest for many of these cells, an order of magnitude of 20 or even greater for δA. One of the important parameters needed, to evaluate β, is G_m, the specific membrane conductance. However, because of the presence of these transport number effects and the invariable presence of multiple time constants, most estimates of R_m are probably gross overestimates. As a starting point therefore, a value of about 5 $k\Omega\ cm^2$ (rather less than estimates such as those by Gorman & Mirolli, 1972) will be chosen for the specific membrane resistance, giving a G_m of $2 \times 10^{-4}\ S \cdot cm^{-2}$. Many of these invaginations are extremely small in diameter (e.g. Plates 2 & 4 in Mirolli & Talbott, 1972) being of the order of 0.3 to 0.4 μm so that $a = 0.2\ \mu m$ (2×10^{-5} cm). For a large 100 μm radius cell it will be assumed that $\ell \cong 50\ \mu m \cong 5 \times 10^{-3}$ cm. Free-solution ion diffusion coefficients are $\sim 10^{-5}\ cm^2 \cdot sec^{-1}$ and $F = 96{,}500$ Coulomb $\cdot$ mole^{-1} and $RT/F = 25.3$ mV at 20°C. for a typical concentration [K] of 10 mM (10^{-5} moles $\cdot$ cm^{-3}), $\beta \cong 1.3$, implying that for $\delta A = 10$ that $\Delta V_m(\infty)/\Delta V_m(0) \cong 1.3$ from Fig. 6. If there were any factors reducing the diffusion coefficient within these narrow invaginations then D might be much less. For example, decreasing D to $10^{-6}\ cm^2 \cdot sec^{-1}$ would increase β to 13 and $\Delta V_m(\infty)/\Delta V_m(0)$ to about 2.7. Similarly if [K] within the invaginations were also less because of active transport pumping, β could increase still further. In fact, increasing G_m or ℓ, or decreasing a, C_o or D has the effect of increasing β. In addition, increasing the value of δA will result in an even greater increase in the magnitude of these slow voltage changes. If, however, the true values of the above parameters for a particular cell are such that $\beta \ll 1$, then transport number effects in membrane invaginations can be assumed to be negligible. When using this analysis it should also be remembered that the analytical predictions have been made on the assumption that the invaginations were of a uniform size and distribution and that the concentration changes remained small enough so that $\ln(1 + \Delta C/C) \sim \Delta C/C$. As illustrated in Fig. 7, violation of this condition will increase the magnitude and rate of onset of slow voltage changes for hyperpolarizing current pulses. Likewise, the addition of an access resistance region at the mouth of any of the invaginations, will also increase the magnitude of these transport number effects. Probably of even more significance, is the presence of a further unstirred layer or region of restricted diffusion surrounding the cell beyond the invaginations, which will also tend to increase the magnitude of these effects.

Using the above cell dimensions with $D = 10^{-5}\ cm^2 \cdot sec^{-1}$, other transport number contributions can also be estimated. From Eq. (41) for such a 100-μm radius cell, slow voltage changes due to average concentration changes within the cell interior can be estimated. In this case $\delta V/\Delta V \sim 8 \times 10^{-4}\ t$ assuming that, as expected with KCl electrodes, $\alpha_t \sim 0.5$. This implies that, for such a cell, significant slow voltage changes will only occur for times $t \gg 1 \times 10^3$ sec. Comparing these changes, with those produced within membrane invaginations, indicates that $R_1 = (\delta V/\Delta V)/\beta \cong 0.6 \times 10^{-3}\ t$ so that they would only be dominant for $t \gg 2000$. If a was 10 times bigger (2 μm), ℓ 5 times smaller (10 μm) and G_m 10 times smaller, these effects would now be dominant for $t \gg 1$ sec.

For some cells there is a restricted diffusion space surrounding the cell. In the squid axon there is a 30-nm (0.03 μm) space between the axon and enclosing Schwann cells (Frankenheuser & Hodgkin, 1956), whereas in the G cell of the nudibranch mollusc (Mirolli & Talbott, 1972) there is only a 20-nm (0.02 μm) space between the large G cell and its surrounding glial cells. Using this latter value and $2 \times 10^{-4}\ S \cdot cm^{-2}$ for G_m implies from Eq. (49) that $\delta V/\Delta V \cong 2.6\ t$, suggesting large slow voltage changes for times $\gtrsim 1$ sec. Comparing this with the predictions of the invaginated membrane transport number effects for $\ell = 50\ \mu m$, $a = 0.2\ \mu m$, $D = 10^{-5}\ cm^2 \cdot sec^{-1}$ results in $R_2 = (\delta V/\Delta V)/\beta = 2t$ implying that both contributions are comparable for times ~ 1 sec. Of course, with both invaginations and a restricted diffusion space occurring together, the boundary condition Eq. (A5) would have to be modified, and the actual concentration changes in the invaginations would be greatly magnified.

For the large bursting cells of *Aplysia,* however, there is apparently no morphological evidence for such a well-defined consistent barrier around the cells (Eaton, 1972). Neher and Lux (1973) have inferred a rather less well-defined diffusion barrier about 20 μm from the cell. In such a case, from Eq. (49), $\delta V/\Delta V \cong 2.6\, t$. This would become significant for times >0.4 sec (equilibration time within the space would be $\gg$0.4 sec).

If the effects of a 0.02 μm restricted diffusion space were compared with an unstirred layer of 200 μm surrounding the cell (assuming α_s is the same in both cases) then the ratio of the two possible contributions R_3/R_2 would be $d\delta/(Dt) = 0.004/t$. For times >4 msec the restricted diffusion case would dominate and in fact, for times less than this, the unstirred-layer case would not have reached a steady state. For a 200-μm unstirred layer compared to a 20-μm sized restricted diffusion space $R_3/R_2 = 4/t$ and hence for times $\geqslant$4 sec the restricted diffusion case would predominate. For times much less than this the ion would not have 'equilibrated' across the restricted diffusion space and neither would the profile in the unstirred-layer case have quite reached a steady state.

If we consider the role of dendrites in producing slow potential changes or in causing a time-dependent decrease in amplitude of some currents, we can still apply exactly the same analysis and parameters except that now δA and β refer to the relative area and properties of the dendrites. For example, such effects may explain the apparent inactivation of some calcium currents. It has been estimated that $\ell \sim 150$ μm, $a \sim 3$ μm for hippocampal pyramidal neurones in guinea pig (Johnston & Brown, 1983), whereas measurements of calcium conductances in chromaffin cells indicate $G_m \sim 4 \times 10^{-4}$ S · cm^{-2} [i.e. 2.4 kΩ · cm^2 from a peak current of 0.22 pA · μm^{-2} in a 1 mM [Ca] solution and a driving force of 52 mV, (Fenwick, Marty & Neher, 1982, Table 2)]. Assuming an internal calcium concentration of 10^{-7} M (10^{-4} moles · cm^{-3} e.g. 10^{-7} to 10^{-8} M; Kostyuk, 1981) and $D_{Ca} \sim 10^{-5}$ cm^2 · sec^{-1} this implies that β will be extremely large, about 1.6×10^5. Provided δA is of reasonable magnitude, this implies very significant changes in $[Ca]_i$ within the dendrites. It should be remembered that, because of the simple boundary condition at the mouth of the invaginations or dendrites, this is particularly likely to underestimate the magnitude of the transport number effects in the dendrites. This could reduce the calcium currents by reducing the driving force on calcium, as in the invagination transport number analysis discussed in this paper, in which the driving force on potassium is reduced, and the magnitude of the effect could then be estimated from values of δA and β. Such a slow, time-dependent decrease in calcium current has indeed been observed and assumed to be an inactivating property of the membrane itself. On the other hand, there seems to be some evidence that there might be a direct effect of $[Ca]_i$ causing inactivation of the current (e.g. Tsien, 1983). In such a case, this could be simply modeled by appropriately modifying Eqs. (5) and (7). Otherwise the basic principles outlined in this paper would still apply. As expected for transport number effects in either case, Fenwick et al. (1982) showed that buffering $[Ca]_i$ with EGTA resulted in a much smaller decline in calcium current with time than in its absence.

Discussion

In this paper it has been shown that the presence of membrane invaginations in a cell can give rise to slow changes in potential during the passage of current across the cell membrane, resulting from differences in ion transport numbers, between the cell membrane and the solution within the invagination, which then give rise to depletion (or enhancement) of the major permeant ion species within the invaginations. Both analytical and numerical solutions have been given and predictions compared. It has been shown that in the case of large currents and potentials the predictions of the analytical solutions will underestimate the magnitudes and rates of onset of the voltage responses. In order to estimate the magnitude of these transport number effects in a given situation it is only necessary to evaluate two nondimensional parameters: the invagination transport number parameter ($\beta = 2G_m RT\ell^2/(aF^2C_oD)$) from Eq. (15) and the relative area occupied by the invaginations $\delta A(= 2\pi na\ell)$ given by Eq. (16). Knowing these two parameters, the magnitude and time course in nondimensional units of the slow potential changes can be estimated from the equation and figures given in this paper and then the time course converted to real units by multiplying nondimensional times by (ℓ^2/D), as in Eq. (13). The fact that β is inversely proportional to C_o immediately suggests, at least in principle, one way of reducing the magnitude of these transport number effects is simply to increase the bathing solution concentration of that ion.

It has also been shown in the previous section that there are various other possible transport number contributions that can result in slow potential changes following the passage of current across a cell membrane. These are changes in the concentration of the major permeant ion which could occur as (1) changes in the average concentration of that ion within the interior of a cell; (2) changes in the average concentration of that ion within a small re-

stricted space surrounding a cell or (3) changes in the interfacial concentration of that ion in the unstirred-layer surrounding a cell. In that previous section it was also shown how the relative magnitude of such other transport number contributions could be assessed from Eqs. (44), (50) and (56).

If the relative concentration changes in membrane invaginations are small, so that Eq. (5) can be linearized to Eq. (7), the predictions will be identical for depletion and enhancement of ions. However, if they are not, then the effects of depletion will be much more significant than those resulting from enhancement.

From order-of-magnitude estimates of morphological and other data for some neuronal cells it is suggested that $\delta A > 10$ and $\beta \sim 1.3$ implying $\Delta V_m(\infty)/\Delta V_m(0) \sim 1.3$. If, however, more correct values of some of those factors used to estimate β were to result in its value increasing, then the magnitude of the predicted slow potential changes would be much greater. For example, if the diffusion coefficient within the membrane invaginations were to be decreased to 10^{-6} cm$^2 \cdot$ sec^{-1} this would increase β to 13 and $\Delta V_m(\infty)/\Delta V_m(0)$ to 2.7. Also, including the effect of any additional unstirred-layer or restricted diffusion space beyond the cells would greatly increase the magnitude of the membrane invagination transport effect component and of course it would also contribute an additional component itself. For the parameters and cell dimensions considered, concentration changes within the cell interior were relatively smaller than in the invaginated regions for all but extremely long times ($\gtrsim$1000 sec). However, for a 20-nm restricted diffusion space for some large cells, which are surrounded by glial cells, it was estimated that this space would result in large slow potential changes ($\delta V/\Delta V \cong 2.6\ t$) for times $t \gtrsim 1$ sec. The additional presence of membrane invaginations would further increase the magnitude of these slow voltage changes. In order to make more accurate estimates of such transport number effects in a particular cell, more detailed and reliable morphological electrophysiological data is required.

It has also been suggested that dendrites are equivalent to reversed invaginations, and that the same analysis can equally apply to them, provided that δA and β now refer to the properties of the dendrites and that the boundary condition at the mouth of the dendrites is still satisfied and is not significantly affected by the finite dimensions of the interior of the cell. As we have seen, because of the low value of $[Ca]_i$ and the length of the dendrites, β will be very large. These transport number effects, therefore, may well help to explain some aspects of the apparent inactivation of calcium currents sometimes observed in cells with a large number of dendrites. An obvious experimental technique to reduce the magnitude of the dendrite transport number effect would be to internally buffer internal calcium with a chelating agent such as EGTA as was done by Fenwick et al. (1982).

The significance of appreciating all these transport number effects is that, if they are not fully taken into account, such slow, time-dependent potential changes or the reduction of ionic current during voltage-clamp experiments could be mistaken for time-dependent changes in membrane permeability, which could lead to very erroneous conclusions about factors controlling ion permeability. In addition, being aware of their magnitude and role in a particular situation will result in the ability to modify this role in some circumstances and to correct for it in others in order to evaluate if there are indeed any residual true permeability changes independent of transport number effects.

I would like to acknowledge the support of the Australian Federal Government CPPER Grant and the Australian Research Grants scheme during the preparation of this paper. I would also like to express my appreciation to Elaine Bonnet and Cynthia Prescott for their help in its preparation and to Professor P.W. Gage and Drs. A.F. Dulhunty, G.D. Lamb and R.E. Wachtel for their helpful comments on the manuscript and to Dr. D.J. Adams, Susan Andrews and Chris French for helpful discussions at different stages of the analysis.

References

Almers, W. 1972. Potassium conductance changes in skeletal muscle and the potassium concentration in the transverse tubules. *J. Physiol. (London)* **225:**33–56

Andrews, S. 1977. A Study of Neurones in Aplysia Abdominal Ganglia. M. Sc. Thesis. University of New South Wales, Sydney, Australia

Barry, P.H. 1977. Transport number effects in the transverse tubular system and their implications for low frequency impedance measurement of capacitance of skeletal muscle fibers. *J. Membrane Biol.* **34:**383–408

Barry, P.H. 1983. The effects of unstirred-layers on the movement of ions across cell membranes. *Proc. Aust. Physiol. Pharmacol. Soc.* **14:**152–169

Barry, P.H., Adrian, R.H. 1973. Slow conductance changes due to potassium depletion in the transverse tubules of frog muscle fibers during hyperpolarizing pulses. *J. Membrane Biol.* **14:**243–292

Barry, P.H., Diamond, J.M. 1984. Effects of unstirred layers on membrane phenomena. *Physiol. Rev.* **64:**763–872

Barry, P.H., Dulhunty, A.F. 1984. Slow potential changes in mammalian muscle fibres during prolonged hyperpolarization: Transport number effects and chloride depletion. *J. Membrane Biol.* **78:**235–248

Barry, P.H., Hope, A.B. 1969*a*. Electroosmosis in membranes: Effects of unstirred layers and transport numbers. I. Theory. *Biophys. J.* **9:**700–728

Barry, P.H., Hope, A.B. 1969*b*. Electroosmosis in membranes: Effects of unstirred layers and transport numbers. II. Experimental. *Biophys. J.* **9:**729–757

Bullock, T.H., Orkand, R., Grinell, A. 1977. Introduction to the Nervous System. W.H. Freeman, San Francisco

Carslaw, H.S., Jaeger, J.C. 1959. Conduction of Heat in Solids. 2nd Edition. Clarendon, Oxford

Coggeshall, R.E. 1967. A light and electron microscope study of the abdominal ganglion of *Aplysia californica*. *J. Neurophysiol.* **13**:1263–1287

Dewhurst, D.J. 1960. Concentration polarization in plane membrane-solution systems. *Trans. Faraday Soc.* **56**:599–609

Eaton, D.C. 1972. Potassium ion accumulation near a pace-making cell of *Aplysia*. *J. Physiol. (London)* **224**:421–440

Fenwick, E., Marty, A., Neher, E. 1982. Sodium and calcium channels in bovine chromaffin cells. *J. Physiol. (London)* **331**:599–635

Frankenheuser, B., Hodgkin, A.L. 1956. The after-effects of impulses in the giant nerve fibres of *Loligo*. *J. Physiol. (London)* **131**:341–376

Gorman, A.L.F., Mirolli, M. 1972. The passive electrical properties of the membrane of a molluscan neurone. *J. Physiol. (London)* **227**:35–49

Graubard, K. 1975. Voltage attenuation within *Aplysia* neurons: The effect of branching pattern. *Brain Res.* **88**:325–332

Jaeger, J.C. 1961. An Introduction to the Laplace Transformation. 2nd Edition. Methuen, London

Johnston, D., Brown, T.H. 1983. Interpretation of voltage-clamp measurements in hippocampal neurons. *J. Neurophysiol.* **50**:464–486

Kostyuk, P.G. 1981. Calcium channels in the neuronal membrane. *Biochim. Biophys. Acta* **650**:128–150

Lakshminarayanaiah, N. 1967. Water transport through cation exchange membranes. *Desalination* **3**:97–105

MacDonald, R.C. 1976. Effects of unstirred layers or transport number discontinuities on the transient and steady-state current-voltage relationships of membranes. *Biochim. Biophys. Acta* **448**:199–219

MacLachlan, N.W. 1953. Complex Variable Theory and Transform Calculus. Cambridge University Press, Cambridge

Mirolli, M., Talbott, S.R. 1972. The geometrical factors determining the electrotonic properties of a molluscan neurone. *J. Physiol. (London)* **227**:19–34

Neher, E., Lux, H.D. 1973. Rapid changes of potassium concentration at the outer surface of exposed single neurons during membrane current flow. *J. Gen. Physiol.* **61**:385–399

Noyes, D.H., Rehm, W.S. 1971. Unstirred layer model for the long time-constant transient voltage response to current in epithelial tissue. *J. Theor. Biol.* **32**:25–45

Orkand, R.K. 1980. Symposium on: Functional Consequences of Ionic Changes Resulting from Electrical Activity. *Fed. Proc.* **39**:1514–1542

Robinson, R.A., Stokes, R.H. 1965. Electrolyte Solutions. Butterworths, London

Segal, J.R. 1967. Electrical capacitance of ion-exchanger membranes. *J. Theor. Biol.* **14**:11–34

Smith, J.R. 1977. Electrical Characteristics of Biological Membranes in Different Environments. Ph.D. Thesis. University of New South Wales, Sydney, Australia

Tsien, R.W. 1983. Calcium channels in excitable cell membranes. *Annu. Rev. Physiol.* **45**:341–358

Valdiosera, R., Clausen, C., Eisenberg, R.S. 1974. Impedance of frog skeletal muscle fibers in various solutions. *J. Gen. Physiol.* **63**:460–491

Wedner, H.J., Diamond, J.M. 1969. Contributions of unstirred-layer effects to apparent electrokinetic phenomena in the gall bladder. *J. Membrane Biol.* **1**:92–108

Received 6 July 1984

Appendix A

Time-Dependent Solution of the Equations Describing the Transport Number Effects in Invaginated Membranes (with Infinite Luminal Conductance)

Using the same symbol notation as in the text, the differential equations [Eqs. (2)–(9)] and boundary conditions, outlined there, will now be solved. From Eqs. (4) and (7), writing V_m for ΔV_m,

$$\frac{\partial C}{\partial t} = \frac{2G_m}{aF}\left[V_m + \frac{RT}{F} - \frac{RTC}{FC_o}\right] + D\frac{\partial^2 C}{\partial x^2}. \tag{A1}$$

Taking Laplace transform of both sides of Eq. (A1) it becomes:

$$D\frac{d^2\bar{C}}{dx^2} - \bar{C}(p + \theta\beta) = -C_o\left\{1 + \theta\beta\left(\eta\bar{V}_m + \frac{1}{p}\right)\right\} \tag{A2}$$

where $\bar{C}(x) = \int_0^\infty e^{-pt}C(x,t)dt$ with a similar definition for $\bar{V}_m$, p is the Laplacian operator, which must be sufficiently large so that the integral converges, and

$$\theta \equiv D/\ell^2 \tag{A3}$$

$$\eta \equiv F/RT. \tag{A4}$$

The boundary equations are now given at $x = 0$ by

$$\bar{C} = C_o/p \tag{A5}$$

and at $x = \ell$ by

$$\left(\frac{d\bar{C}}{dx}\right)_{x=\ell} = 0. \tag{A6}$$

The full solution to Eq. (A2) may be shown to be given by

$$\bar{C} = \bar{C}_o(p) + K_1e^{qx} + K_2e^{-qx} \tag{A7}$$

where

$$\bar{C}_o(p) \equiv \frac{C_o\left[1 + \theta\beta\left(\eta\bar{V}_m + \frac{1}{p}\right)\right]}{(p + \theta\beta)} \tag{A8}$$

$$q \equiv [(p + \theta\beta)/D]^{1/2} \tag{A9}$$

and K_1 and K_2 are the two constants of integration, which may be evaluated from the boundary condition to give

$$\bar{C} = \bar{C}_o(p) + \left[\frac{C_o}{p} - \bar{C}_o(p)\right]\frac{\cosh q(x - \ell)}{\cosh q(\ell)}. \tag{A10}$$

Taking the Laplace transforms also of Eqs. (7) and (9) we obtain

$$\bar{i}_o = 2\pi a\int_0^\ell \bar{i}_K dx = 2\pi a\int_0^\ell\left[-\frac{G_m}{\eta}\left(\eta\bar{V}_m + \frac{1}{p} - \frac{\bar{C}}{C_o}\right)\right]dx. \tag{A11}$$

Substituting for $\bar{C}$ from Eq. (A10) into Eq. (A11), multiplying by

n, the number of invaginations per cm^2 of surface membrane, and simplifying we obtain

$$n\bar{i}_o = -\delta A \cdot G_m \bar{V}_m \left[\frac{p}{(p+\theta\beta)} + \frac{\theta\beta}{(p+\theta\beta)} \frac{\tanh(q\ell)}{q\ell}\right] \tag{A12}$$

where δA, representing the relative area of the invaginated membrane region, is again given by

$$\delta A = 2\pi n a \ell. \tag{A13}$$

The Laplace transform of Eq. (10) is

$$\bar{i}_t = n\bar{i}_o - \bar{V}_m G_m \tag{A14}$$

and hence substituting for $n\bar{i}_o$ from Eq. (A12) in Eq. (A14) and expressing in terms of $\bar{V}_m$ we obtain

$$\bar{V}_m = \frac{-\bar{i}_t R_m (p+\theta\beta)}{\left[p(1+\delta A) + \theta\beta\left(1 + \delta A \frac{\tanh(q\ell)}{q\ell}\right)\right]}. \tag{A15}$$

For a constant current pulse of amplitude I

$$\bar{i}_t = I/p. \tag{A16}$$

Substituting for $\bar{i}_t$ from Eq. (A16) into Eq. (A15) and using the Laplace inversion theorem (e.g. Jaeger, 1961) we obtain

$$V_m = -\frac{IR_m}{2\pi i}\int_{\gamma-i\infty}^{\gamma+i\infty} \frac{(p+\theta\beta)e^{pt}dp}{p\left[p + \theta\beta + \delta A\left(p + \theta\beta\frac{\tanh ql}{ql}\right)\right]} \tag{A17}$$

where again $i = \sqrt{-1}$ and where δ is chosen such that all the poles lie to the left of the line $\gamma + i\infty$, $\gamma - i\infty$. Making the following transformation

$$\begin{aligned} &\lambda = p + \theta\beta \qquad && \frac{d\lambda}{d\mu} = 2\mu \\ &\mu = \sqrt{\lambda} \\ &dp = d\lambda && q\ell = (\lambda/\theta)^{1/2} \end{aligned} \tag{A18}$$

$$V_m = -\frac{IR_m}{2\pi i}\int_{\gamma'-i\infty}^{\gamma'+i\infty} \frac{\lambda e^{(\lambda-\theta\beta)t}d\lambda}{(\lambda-\theta\beta)\left[\lambda + \delta A\left(\lambda + \theta\beta\left(\frac{\tanh q\ell}{q\ell} - 1\right)\right)\right]} \tag{A19}$$

where γ' is chosen in Eq. (A19) to fulfill the same criterion as for γ in Eq. (A17). Evaluating this integral is formally equivalent to evaluating $2\pi i$ times the sums of the residues of the poles of this integrand.

There are 3 possible sets of poles.

(i) When $\lambda = \theta\beta$, the residue is simply

$$\frac{1}{1 + \delta A(\tanh\sqrt{\beta})/\sqrt{\beta}}. \tag{A20}$$

(ii) There is a pole for $\lambda = \theta\alpha^2$ where $\alpha^2 < \beta$ which occurs as the root of

$$\alpha^2 + \delta A\left[\alpha^2 + \beta\left(\frac{\tanh\alpha}{\alpha} - 1\right)\right] = 0 \tag{A21}$$

as already given in Eq. (18) in the text.

Using the residue formula (MacLachlan, 1953; p. 54) it may be shown that if there is a pole at $\lambda = a$ and the integrand of the function requiring transformation is of the form $N(\lambda)/D(\lambda)$ then, provided $N(a)$ is nonzero, the residue is $N(a)/D'(a)$ where $D'(a)$ is the differential of $D(a)$. These conditions are met in Eq. (A19) and hence the residue becomes

$$\frac{\alpha^2 e^{(\alpha^2-\beta)\theta t}}{(\alpha^2-\beta)[Z_1(\alpha) + Z_2(\alpha)\tanh\alpha]} \tag{A22}$$

where

$$Z_1(\alpha) \equiv 1 + \delta A + \frac{\delta A \cdot \beta}{2\alpha^2} \tag{A23}$$

and

$$Z_2(\alpha) \equiv \frac{\alpha}{2}(1+\delta A) - \frac{\delta A \cdot \beta}{2\alpha^3}(1+\alpha^2) \tag{A24}$$

as in Eqs. (19) and (20) in the text.

(iii) Similarly there is an infinite number of poles given by $\lambda = -\theta\alpha_m^2$. These poles occur as the roots of

$$\alpha_m^2 + \delta A\left[\alpha_m^2 - \beta\left(\frac{\tan\alpha_m}{\alpha_m} - 1\right)\right] = 0 \tag{A25}$$

as in Eq. (22) in the text.

As before in (ii) the residues of these poles may be evaluated using the residue formula as

$$\frac{\alpha_m^2 e^{-(\alpha_m^2+\beta)\theta t}}{(\alpha_m^2+\beta)[Z_1(i\alpha_m) + iZ_2(i\alpha_m)\tan\alpha_m]} \tag{A26}$$

where

$$Z_1(i\alpha_m) = 1 + \delta A - \frac{\delta A \cdot \beta}{2\alpha_m^2} \tag{A27}$$

and

$$iZ_2(i\alpha_m) = \frac{\alpha_m}{2}(1+\delta A) + \frac{\delta A \cdot \beta}{2\alpha_m^3}(1-\alpha_m^2) \tag{A28}$$

as in Eqs. (23) and (24) in the text.

If we add $2\pi i$ times the sums of the residues given by Eqs. (A20), (A22) and (A26) along with their subsidiary equations this gives the solution to the integral in Eq. (A19). If we further redefine time t in terms of the nondimensional time parameter T' by

$$T' = \theta t = Dt/\ell^2 \tag{A29}$$

the solution to Eq. (A15) in ordinary space becomes:

$$\frac{\Delta V(T')}{\Delta V(0)} = (1+\delta A)\left[A_1(\beta) + A_2(\alpha,\beta)e^{-(\alpha^2-\beta)T'} + \sum_{m=1}^{\infty} A_2(i\alpha_m,\beta)e^{-(\alpha_m^2+\beta)T'}\right] \tag{A30}$$

where

$$A_1(\beta) = \frac{1}{1 + \delta A \cdot (\tanh \sqrt{\beta})/\sqrt{\beta}} \quad \text{(A31)}$$

$$A_2(\alpha,\beta) = \frac{\alpha^2}{(\alpha^2 - \beta)[Z_1(\alpha) + Z_2(\alpha) \tanh \alpha]} \quad \text{(A32)}$$

$$A_2(i\alpha_m,\beta) = \frac{\alpha_m^2}{(\alpha_m^2 + \beta)[Z_1(i\alpha_m) + iZ_2(i\alpha_m) \tan \alpha_m]} \quad \text{(A33)}$$

$$Z_1(\alpha) \equiv 1 + \delta A + \frac{\delta A \cdot \beta}{2\alpha^2} \quad \text{(A34)}$$

$$Z_2(\alpha) = \frac{\alpha}{2}(1 + \delta A) - \frac{\delta A \cdot \beta}{2\alpha^3}(1 + \alpha^2) \quad \text{(A35)}$$

where $i \equiv \sqrt{-1}$ and $Z_1(i\alpha_m)$ and $Z_2(i\alpha_m)$ are simply obtained by substituting $i\alpha_m$ for α in Eqs. (A34) and (A35). Eqs. (A29)–(A35) are the same as Eqs. (11)–(14) and (17)–(24) in the text.

Appendix B

Steady-State Solution of the Equations Describing Transport Number Effects in Invaginated Membranes (with Finite Luminal Conductivity)

Further simplifying the equations in the text and converting them completely to nondimensional form the full time-dimensional equations become

$$\frac{\partial C'}{\partial T'} = -\beta I_K + \frac{\partial^2 C'}{\partial X^2} \quad \text{(B1)}$$

$$I_K = -(\varepsilon_m - \varepsilon - \ln C) = Fi_K/RTG_m \quad \text{(B2)}$$

$$\frac{d\varepsilon}{dX} = -\frac{\beta \cdot \Theta}{\delta A} \cdot I(X) \quad \text{(B3)}$$

$$I_K = -\frac{1}{\delta A} \cdot \frac{dI}{dX} \quad \text{(B4)}$$

$$I_t = I_o - \varepsilon_m \quad \text{(B5)}$$

where

$$C' = C/C_o \qquad X = x/\ell \quad \text{(B6)}$$

$$\varepsilon = FV/RT \qquad \varepsilon_m = FV_m/RT \quad \text{(B7)}$$

$$I_o = \frac{nFi_o}{G_mRT} \qquad I(X) = \frac{nFi(x)}{G_mRT} \quad \text{(B8)}$$

$$I_t = \frac{Fi_t}{G_mRT} \qquad \Theta = \frac{DF^2C_o}{RTG_L} \quad \text{(B9)}$$

and where β and δA are as previously defined by Eqs. (15) and (16).

In the steady state Eq. (B1) becomes

$$\frac{d^2C'}{dX^2} = \beta I_K. \quad \text{(B10)}$$

Using Eq. (B10) together with Eqs. (B3) and (B4) it follows that

$$\frac{d^2\varepsilon}{dX^2} = \Theta \frac{d^2C'}{dX^2}. \quad \text{(B11)}$$

Integrating twice and using the two boundary conditions that when $X = 0$, $C' = 1$, $\varepsilon = 0$ and when $X = 1$, $dC'/dX = 0$, $d\varepsilon/dX = 0$ the simple relationship between potential and concentration within the invaginations is obtained

$$\varepsilon = \Theta(C' - 1). \quad \text{(B12)}$$

Linearizing the logarithm term in Eq. (B2) and substituting for ε from Eq. (B12) the equation becomes

$$I_K = -[\varepsilon_m + (\Theta + 1) - C'(\Theta + 1)]. \quad \text{(B13)}$$

From Eqs. (B10) and (B13) the concentration differential equation becomes

$$\frac{d^2C'}{dX^2} = -\beta[\varepsilon_m + (\Theta + 1)] + \beta(\Theta + 1)C'. \quad \text{(B14)}$$

It may readily be shown that the general solution of this differential equation is

$$C' = A_1 e^{\sqrt{\beta'}X} + A_2 e^{-\sqrt{\beta'}X} + [1 + \varepsilon_m/(\Theta + 1)] \quad \text{(B15)}$$

where A_1 and A_2 are constants of integration and β' is given by

$$\beta' = \beta(\Theta + 1). \quad \text{(B16)}$$

Using the boundary conditions for $X = 0$, $(C' = 1)$ and $X = 1$, $(dC'/dX = 0)$ the solution becomes:

$$(C' - 1) = \frac{\varepsilon_m}{(\Theta + 1)}\left[1 - \frac{\cosh[\sqrt{\beta'}(X - 1)]}{\cosh \sqrt{\beta'}}\right]. \quad \text{(B17)}$$

From Eqs. (B12) and (B17) together with Eqs. (B3) and (B16)

$$I(X) = \frac{\delta A}{\sqrt{\beta'}} \varepsilon_m \frac{\sinh[\sqrt{\beta'}(X - 1)]}{\cosh \sqrt{\beta'}}. \quad \text{(B18)}$$

Hence

$$I_o = I(0) = -\frac{\delta A}{\sqrt{\beta'}} \varepsilon_m \tanh \sqrt{\beta'}. \quad \text{(B19)}$$

From Eqs. (B5) and (B19) in the steady state

$$-\frac{V_m}{iR_m^*} = -\frac{\varepsilon_m(1 + \delta A)}{I_t} = \frac{(1 + \delta A)}{1 + \delta A (\tanh \sqrt{\beta'})/\sqrt{\beta'}}. \quad \text{(B20)}$$

Now even in the absence of transport number effects, a finite value of Θ results in a drop in voltage down the invagination so that the initial value of $-V_m/iR_m^*$ is no longer 1.0. This initial value can be readily obtained by solving Eqs. (B2)–(B4) with $C = 1$, so that Eq. (B2) becomes

$$I_K = -(\varepsilon_m - \varepsilon). \quad \text{(B21)}$$

From Eqs. (B21), (B3) and (B4) the differential equation becomes

$$\frac{d^2\varepsilon}{dX^2} = -\beta\Theta(\varepsilon_m - \varepsilon). \tag{B22}$$

Following exactly the same procedure as for the solution of Eq. (B14), with $\varepsilon = 0$ when $X = 0$ and $d\varepsilon/dX = 0$ when $X = 1$, the solution becomes

$$I_o = \frac{\delta A \cdot \varepsilon_m}{\sqrt{\beta\Theta}} \tanh \sqrt{\beta\Theta}. \tag{B23}$$

Hence from Eq. (B5)

$$-\frac{\varepsilon_m}{I_t} = \frac{1}{1 + \delta A\,(\tanh \sqrt{\beta\Theta})/\sqrt{\beta\Theta}} \tag{B24}$$

so that initially

$$-\frac{V_m}{iR_m^*} = -\frac{\varepsilon_m}{I_t}(1 + \delta A) = \frac{1 + \delta A}{1 + \delta A\,(\tanh \sqrt{\beta\Theta})/\sqrt{\beta\Theta}} \tag{B25}$$

and hence from Eqs. (B20) and (B25)

$$\frac{\Delta V(\infty)}{\Delta V(0)} = \frac{1 + \delta A\,(\tanh \sqrt{\beta\Theta})/\sqrt{\beta\Theta}}{1 + \delta A\,(\tanh \sqrt{\beta'})/\sqrt{\beta'}}. \tag{B26}$$

For small values of Θ, $\beta' \to \beta$ and Eq. (B20) becomes equivalent to Eq. (25) in the text. Even larger values of Θ only serve to increase the effective magnitude of the transport number parameter. For typical physiological solutions ($D = 1.5 \times 10^{-5}$ cm $\cdot$ ^{2} $\cdot$ sec^{-1}, $C_o = 5 \times 10^{-6}$ mol $\cdot$ cm^{-3}, $G_L = 10^{-2}$ S $\cdot$ cm^{-1}) it may be calculated from Eq. (B9) that $\Theta \cong 0.03$. Thus this represents a 3% correction to β. As may be noticed from that equation, Θ is quite independent of invagination geometry although $\Theta\beta$ is not [*see* Eq. (29b)].

Appendix C

Numerical Analysis of Transport Number Equations for an Invaginated Membrane

Dropping the prime from C' and T', the equations in Appendix B can be readily rewritten in a form suitable for numerical analysis. Consider the invaginations to be divided into NX elements of thickness DX.

Given a value of total current IT an initial estimate of the membrane potential parameter EM is obtained from

$$\text{EM} = -\text{IT}/(1 + \text{DELA}) \tag{C1}$$

where EM, IT and DELA are equivalent to ε_m, I_t and δA in Eqs. (B7)–(B9) in Appendix B and Eq. (16) in text. Using this initial value of EM, the currents and potentials down the Nth element of the invaginations will be given (writing in Fortran language style) from Eqs. (B2)–(B5) by

$$\text{DE(N)} = -\text{BETA*THETA*I(N} - 1)\text{*DX/DELA} \tag{C2}$$

$$\text{E(N)} = \text{E(N} - 1) + \text{DE(N)}. \tag{C3a}$$

For the first and Nth elements,

$$\text{E(1)} = \text{DE(1)}/2 \tag{C3b}$$

$$\text{IK(N)} = -\{\text{EM} - \text{E(N)} - \text{LN[C(N)]}\} \tag{C4}$$

$$\text{DI(N)} = -\text{IK(N)*DELA*DX} \tag{C5}$$

$$\text{I(N)} = \text{I(N} - 1) + \text{DI(N)} \tag{C6}$$

where

$$\text{DX} = 1.0/\text{NX}. \tag{C7}$$

BETA, THETA, IK and E are the same as β,Θ, I_K and ε in Appendix B and I(0) = I_o, E(0) = 0 and * represents multiplication. LN[C(N)] is either $\log_e$[C(N)], or C(N) − 1 for the linear approximation, C(N) being the relative ionic concentration within the Nth element. If the correct value of ε_m were to be chosen, the current, I(NX), at the closed end of the invagination (X = 1), should be zero. A simple, very rapidly converging, iterative correction was obtained by changing EM in a way which was equivalent to reducing the current entering the invagination by I(NX), i.e.

$$\text{EM} = \text{EM} - \text{I(NX)}/(1 + \text{DELA}). \tag{C8}$$

Using this current the concentration change of the first (closest to the surface), Nth and last element will be given by

$$\text{DC(1)} = -\text{BETA*IK(1)} + [\text{C(2)} + 2 - 3\text{*C(1)}]/(\text{DX*DX}) \tag{C9}$$

$$\text{DC(N)} = -\text{BETA*IK(N)} + [\text{C(N} + 1) + \text{C(N} - 1) - 2\text{*C(N)}]/(\text{DX*DX}) \tag{C10}$$

$$\text{DC(NX)} = -\text{BETA*IK(NX)} + [\text{C(NX} - 1) - \text{C(NX)}]/(\text{DX*DX}) \tag{C11}$$

and for each element

$$\text{C(N)} = \text{C(N)} + \text{DC(N)*DT} \tag{C12}$$

where DT is the time step.

The actual computations were done in double precision on a PDP-11/34 computer using the Fortran IV language. For reasonable accuracy either 50 or 100 elements were used with a time step of 0.0002 or 0.00005. Although, simple numerical integration of the above equations really converged remarkably well, the fourth-order Runge-Kutta technique was used to further increase computational accuracy (for further details *see* e.g. p. 270 of Barry & Adrian, 1973). Using the linear log approximation and zero luminal resistance these computed values were found to be within 0.03 and 0.01% of the analytical values for 50 and 100 elements with $\beta = 10$ and $\delta A = 10$.